Signal photon flux and background noise in a coupling electromagnetic detecting system for high-frequency gravitational waves

Fangyu Li,[1,*] Nan Yang,[1,†] Zhenyun Fang,[1,‡] Robert M. L. Baker, Jr.,[2,§] Gary V. Stephenson,[3,‖] and Hao Wen[1,¶]

[1]*Department of Physics, Chongqing University, Chongqing 400044, People's Republic of China*
[2]*GRAWAVE® LLC, 8123 Tuscany Avenue, Playa del Rey, California 90293, USA*
[3]*Seculine Consulting, P.O. Box 925, Redondo Beach, California 90277, USA*

A coupling system among Gaussian-type microwave photon flux, a static magnetic field, and fractal membranes (or other equivalent microwave lenses) can be used to detect high-frequency gravitational waves (HFGWs) in the microwave band. We study the signal photon flux, background photon flux, and the requisite minimal accumulation time of the signal in the coupling system. Unlike the pure inverse Gertsenshtein effect (G effect) caused by the HFGWs in the gigahertz band, the electromagnetic (EM) detecting scheme proposed by China and the U.S. HFGW groups is based on the composite effect of the synchroresonance effect and the inverse G effect. The key parameter in the scheme is the first-order perturbative photon flux (PPF) and not the second-order PPF; the distinguishable signal is the transverse first-order PPF and not the longitudinal PPF; the photon flux focused by the fractal membranes or other equivalent microwave lenses is not only the transverse first-order PPF but the total transverse photon flux, and these photon fluxes have different signal-to-noise ratios at the different receiving surfaces. Theoretical analysis and numerical estimation show that the requisite minimal accumulation time of the signal at the special receiving surfaces and in the background noise fluctuation would be $\sim 10^3$–10^5 seconds for the typical laboratory condition and parameters of $h_{\rm rms} \sim 10^{-26}$–$10^{-30}/\sqrt{\rm Hz}$ at 5 GHz with bandwidth ~ 1 Hz. In addition, we review the inverse G effect in the EM detection of the HFGWs, and it is shown that the EM detecting scheme based only on the pure inverse G effect in the laboratory condition would not be useful to detect HFGWs in the microwave band.

I. INTRODUCTION

The first mention of high-frequency gravitational waves (HFGWs) was during a lecture in 1961 by Forward [1]. The lecture was based upon a paper concerning the dynamics of gravity and Forward's work on the Weber bar. The first actual publication concerning HFGWs was in mid 1962 when Gertsenshtein [2] authored the pioneering paper entitled "Wave Resonance of Light and Gravitational Waves" [it is often called the Gertsenshtein (G) effect]. The next publication was in August of 1964 when Halpern and Laurent [3] suggested that at some earlier stage of development of the Universe (the big bang) conditions were suitable to produce strong relic gravitational radiation. They then discuss "short wavelength" or HFGWs and even suggest a "laser" generator of HFGWs analogous to a laser for electromagnetic (EM) "generation." In 1968, Isaason authored papers [4,5] concerned with "Gravitational Radiation in the Limit of High Frequency."

*cqufangyuli@hotmail.com
†cquyangnan@cqu.edu.cn
‡zyf@cqu.edu.cn
§DrRobertBaker@GravWave.com
‖seculine@gmail.com
¶wenhaowww@yahoo.com.cn

Grishchuk and Sazhin in the period of 1974–1975 discussed a scheme on "Emission of Gravitational Waves by an Electromagnetic Cavity and Detection" [6,7], which also involved HFGWs. In 1974, Chapline, Nuckolls, and Wood [8] suggested the generation of HFGWs by nuclear explosions, and, in 1978, Braginsky and Rudenko discussed detection and generation of HFGWs [9]. In 1979, Hawking and Israd [10] presented an actual definition for HFGWs having frequencies in excess of 100 KHz. However, genuine attention to HFGWs occurred from the 1990s for the following reasons:

(1) The maximal signal and peak of the relic GWs, expected by the quintessential inflationary models [11–15] and some string cosmology scenarios [16–18], may be firmly localized in the gigahertz band, and their root-mean-square (rms) values of the dimensionless amplitudes might reach up to $\sim 10^{-30}$–$10^{-33}/\sqrt{\rm Hz}$. Such works continue today.

(2) The thermal motion of the plasma of stars, the interaction of the EM waves with interstellar plasma and magnetic fields, and the evaporation of primordial back holes [19] are possible means to generate HFGWs.

(3) Study of the nanopiezoelectric resonator scheme [20], the high-energy particle beam [21–25], and

the construction of the LHC [26] are possible methods to produce HFGWs. Their frequencies may reach up to 10^9 Hz and higher.

(4) Some HFGW detectors have already been constructed, and more have been proposed. The constructed HFGW detectors include a toroidal waveguide scheme [27,28] and a coupled superconducting spherical cavities system [29,30]. Proposed detecting schemes include small laser interferometer detectors [31] and the coupling system of a Gaussian beam, static magnetic and fractal membranes [32]. In Table I, we list some possible HFGW sources and their major mechanisms.

In this paper, our attention is focused on signal photon flux, the background photon flux (BPF), and their signal-to-noise ratios in the coupling EM detection scheme. We compute the signal photon fluxes and the signal-to-noise ratios and discuss displaying condition and the requisite minimal accumulation time of the signal in the background noise fluctuation. In addition, we review the inverse G effect in the EM detection of the HFGWs. It is shown that the pure inverse G effect in the laboratory condition cannot by itself detect the expected HFGWs, but the current EM detecting scheme might greatly improve detecting sensitivity and narrow the gap between the theoretical estimation of the expected HFGWs and the possibility of their detection.

The outline of this paper is the following: In Sec. I, we present a brief history of the HFGW research, including analyses of some possible HFGW sources. In Sec. II, we review the detecting scheme based on the pure inverse G effect. In Sec. III, we discuss the EM perturbation generated by the HFGW in a coupling system between the static magnetic and the plane EM wave. In Sec. IV, we study the EM perturbative effect of the HFGW in the coupling system among the Gaussian-type microwave photon flux, the static magnetic field, and the fractal membranes (or other equivalent microwave lenses) and give theoretical analysis, numerical estimations, and a brief review of the role of the fractal membranes or other equivalent microwave lenses. Our conclusions are summarized in Sec. V.

II. DETECTING SCHEME BASED ON THE INVERSE GERTSENSHTEIN EFFECT

It is well known that if an electromagnetic wave (EMW) propagates in a transverse homogeneous static magnetic field, it can generate the gravitational wave (GW). This is just the G effect [2]. Then the converting probability of the EMW (photons) into the GW (graviton) is given by [33,34] (in cgs units)

$$P \approx 4\pi G B^2 L^2/c^4, \tag{1}$$

where G is Newton's gravitational constant and B is the

TABLE I.   Some possible HFGW sources and relevant parameters.

Sources	Amplitude	Frequency	Characteristic
HFGWs in the quintessential inflationary models [11–15]	$h_{\rm rms} \sim 10^{-30}$–$10^{-32}/\sqrt{\rm Hz}$	$\nu \sim 10^9$–10^{10} Hz	Random background
HFGWs in some string cosmology scenarios [16–18]	$h_{\rm rms} \sim 10^{-30}$–$10^{-34}/\sqrt{\rm Hz}$	$\nu \sim 10^8$–10^{11} Hz	Random background
Solar plasma [19]	$h_{\rm rms} \sim 10^{-39}/\sqrt{\rm Hz}$	$\nu \sim 10^{15}$ Hz	On the Earth
High-energy particles (e.g., Fermi ring) [24]	$h_{\rm rms} \sim 10^{-39}$–$10^{-41}/\sqrt{\rm Hz}$	$\nu \sim 10^4$ Hz–10^5 Hz	On the center, the frequency depends on the rotating frequency of the particles in the Fermi ring
Stanford Linear Collider [21]	$h_{\rm rms} \sim 10^{-39}/\sqrt{\rm Hz}$	$\nu \sim 10^{23}$ Hz	On the collision center, the frequency depends on the self-energy and the Lorentz factor of high-energy $e^+ e^-$ beams
The LHC [26]			This is a continuous spectra of high-frequency gravitons, and only integrals for the total spectra distribution range might provide an indirect effect.
Nanopiezoelectric crystal array (size of ∼100 m) [20]	$h_{\rm rms} \sim 10^{-28}$–$10^{-31}/\sqrt{\rm Hz}$	$\nu \sim 10^9$–10^{10} Hz	On the wave zone, an effective cross section of the gravitational radiation would be less than 0.01 m^2

static magnetic field. Contrarily, if a GW passes through a transverse homogeneous static magnetic field, then it can generate an EMW (photon flux), which propagates only in the same and in the opposite propagating directions of the GW. The latter is weaker than the former or is absent. This is just the pure inverse G effect [33,35]. Whether the G effect or its inverse effect, the conversion rate between the GWs (gravitons) and the EMWs (photons) is extremely low. For example, if $B = 10$ T $= 10^5$ G and $L = 10$ m $= 1000$ cm, from Eq. (1), we have

$$P \approx 1.0 \times 10^{-32}. \tag{2}$$

For the EM perturbative effect caused by the GWs in the EM fields, one's attention is often focused to the inverse G effect. In order to consider the pure inverse G effect in the laboratory size, the wavelength of GWs should be the comparable with the laboratory dimension. Thus the HFGWs in the microwave band ($\sim 10^8$–10^{10} Hz) would be suitable researching objects. In fact, the physical foundation of the G effect is the Einstein-Maxwell equations in the weak field condition, while the physical foundation of the inverse G effect is classical electrodynamics in curved spacetime. If a circular polarized HFGW passes through the transverse homogenous static magnetic field, according to the electrodynamical equations in curved spacetime, the EMW produced by the interaction of the HFGW with the static magnetic field can be given by [32,35] (in order to compare possible experimental effects, from now, we use mks units)

$$\vec{E}^{(1)} \approx A\hat{B}_y^{(0)} k_g cz \exp[i(k_g z - \omega_g t)], \tag{3}$$

$$\vec{B}^{(1)} \approx A\hat{B}_y^{(0)} k_g z \exp[i(k_g z - \omega_g t)], \tag{4}$$

where $\vec{E}^{(1)}$ and $\vec{B}^{(1)}$ are parallel to the xy plane and $\vec{E}^{(1)} \perp \vec{B}^{(1)}$. We also assume $A = A_\oplus = A_\otimes = |h_\oplus| = |h_\otimes|$, as the
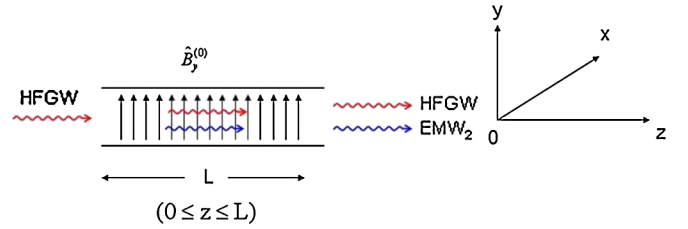

FIG. 1 (color online). If a HFGW passes through a static magnetic field $\hat{B}_y^{(0)}$, the interaction of the HFGW with the static magnetic field will produce an EMW, where L is the interacting dimension between the HFGW and the static magnetic field. The EMW$_2$ has a maximum in the terminal position ($Z = L$) of the interacting volume due to the space accumulation effect in the propagating direction (the z direction).

amplitudes of the HFGW with two polarization states, the superscript (0) denotes the background EM fields, and the notation ˆ indicates the static EM fields. Here we neglected the EMW propagating along the negative direction of the z axis, because it is often much less than the EMW propagating along the positive direction of the z axis. Equations (3) and (4) show that such perturbative EM fields have a space accumulation effect ($\propto z$) in the interacting region: This is because the GWs (gravitons) and EMWs (photons) have the same propagating velocity in a vacuum, so that the two waves can generate an optimum coherent effect in the propagating direction [33,35]. From Eqs. (3) and (4), the power flux density of the EMW in the terminal receiving surface ($z = L$) will have a maximum ($z = L$; see Fig. 1)

$$u_{em} = 1/\mu_0 \cdot |\vec{E}^{(1)} \times \vec{B}^{(1)}| \approx 1/\mu_0 \cdot (A\hat{B}_y^{(0)} k_g L)^2 c. \tag{5}$$

In order to compare and analyze the EM perturbative effect under typical laboratory conditions, we chose the following typical parameters:

$$\hat{B}_y^{(0)} = 10 \text{ T}, \qquad L = 10 \text{ m},$$

$$\nu_e = \nu_g = 5 \text{ GHz} \qquad \left(\lambda_g = 0.06 \text{ m}, \quad k_e = k_g = \frac{2\pi}{\lambda} \approx 100\right),$$

$$h\nu = 3.3 \times 10^{-24} \text{ J (energy of a single photon)},$$

$$A \approx h_{rms} = \hat{h} = 10^{-26}/\sqrt{Hz} \text{ to } 10^{-30}/\sqrt{Hz},$$

$$\Delta s = 0.1 \times 0.1 = 0.01 \text{ m}^2 \text{ (typical receiving surface)}, \tag{6}$$

where Δs is also the cross section of the interacting region. If $\hat{h} = h_{rms} = 10^{-30}/\sqrt{Hz}$, then the total power flux passing through Δs in the terminal position ($z = L$) is

$$U_{em}^{(2)} = u_{em}\Delta s = \frac{1}{\mu_0}(A\hat{B}_y^{(0)} k_g L)^2 c\Delta s \approx 2.3 \times 10^{-40} \text{ W}, \tag{7}$$

where the superscript (2) denotes the second-order perturbative EM power flux. Therefore, the corresponding second-order perturbative photon flux (in quantum language) will be

$$N_\gamma^{(2)} = U_{em}^{(2)}/\hbar\omega_e \approx 2.3 \times 10^{-40}/3.3 \times 10^{-24}$$

$$\approx 7.0 \times 10^{-17} \text{ s}^{-1}. \tag{8}$$

For a HFGW of $\nu_g = 5$ GHz and $\hat{h} = 10^{-30}/\sqrt{\text{Hz}}$, the total power flux passing through the Δs is given by [36]

$$U_{gw} = u_{gw}\Delta s = \frac{c^3}{8\pi G}\omega^2 A^2 \Delta s \approx 1.6 \times 10^{-7} \text{ W}. \quad (9)$$

Thus corresponding graviton flux would be

$$N_g = U_{gw}/\hbar\omega \approx 4.8 \times 10^{16} \text{ s}^{-1}. \quad (10)$$

Because the power flux Eq. (7) [including the photon flux, Eq. (8)] is proportional to the amplitude squared of the HFGW, the second-order perturbative photon flux (PPF) exhibits a very small value.

From Eqs. (7)–(10), we obtain the conversion rate of the HFGW (gravitons) into the EMW (photons) as follows:

$$P \approx U_{em}/U_{gw} = N_\gamma/N_g = \frac{2.3 \times 10^{-40}}{1.6 \times 10^{-7}} = \frac{7 \times 10^{-17}}{4.8 \times 10^{16}}$$
$$\approx 1.4 \times 10^{-33}. \quad (11)$$

Equations (2) and (11) show that the conversion rates of the

EMW (photons) into the HFGW (gravitons) and the contrary process have similar orders of magnitude. Thus, in order to obtain a second-order perturbative photon, from Eq. (8), the signal accumulation time would be at least

$$\Delta t \approx 1/N_r^{(2)} \approx \frac{1}{7 \times 10^{-17}} \approx 1.4 \times 10^{16} \text{ s}. \quad (12)$$

This is a very huge time interval. Equations (11) and (12) also show that the conversion rate of the HFGW (gravitons) into the EMW (photons) is extremely low. Thus the PPF in the pure inverse G effect cannot cause a detectable signal or observable effect in the laboratory condition. Nevertheless, for some astrophysical and cosmological processes, it is possible to cause interesting phenomena, because the very large EM fields (including plasma) and very strong GWs (including low-frequency GWs) often occur simultaneously and these fields extend over a very large area [15,37,38].

From Eqs. (5), (7), (8), and (12), one finds

$$\text{if } \hat{h} = 10^{-26}/\sqrt{\text{Hz}}, \quad \text{then } N_\gamma^{(2)} \approx 7 \times 10^{-9} \text{ s}^{-1} \quad \text{and} \quad \Delta t \approx 1.4 \times 10^8 \text{ s};$$
$$\text{if } \hat{h} = 10^{-24}/\sqrt{\text{Hz}}, \quad \text{then } N_\gamma^{(2)} \approx 7 \times 10^{-5} \text{ s}^{-1} \quad \text{and} \quad \Delta t \approx 1.4 \times 10^4 \text{ s}. \quad (13)$$

Such results show that, even if $\hat{h} = 10^{-24}/\sqrt{\text{Hz}}$, it is still difficult to detect the HFGWs by the inverse G effect in the laboratory condition. In other words, in order to generate an observable effect in such an EM system, the amplitude of the HFGW of $\nu_g = 5$ GHz must be larger than $\hat{h} = 10^{-24}/\sqrt{\text{Hz}}$ at least. Unfortunately, so far as we know, there are no HFGWs as strong as $\hat{h} = 10^{-24}/\sqrt{\text{Hz}}$ or larger, though the EM system based on the pure inverse G effect in the high-vacuum and ultralow-temperature condition has a very good low noise environment. Therefore the EM detecting scheme based on the pure inverse G effect in the laboratory condition would not be available to detect HFGWs in the microwave band.

III. THE PERTURBATIVE PHOTON FLUXES IN COUPLING SYSTEM BETWEEN THE STATIC MAGNETIC FIELD AND THE PLANE EMW

The classical and semiclassical description and linear quantum theory all showed [33,39] that the interaction cross section between the GW (gravitons) and the EMW (photons) in a strong background static magnetic field (virtual photons) will be much larger than that in the pure inverse G effect. In other words, the strong background static magnetic field provides a catalyst to greatly enhance the resonant effect between the EMW (the photons) and the GW (gravitons). However, the presence of a background EMW (the background photon flux) will generate a large photon flux noise. If the PPF (i.e., signal photon flux) and the BPF have the same or very similar

physical behaviors (e.g., propagating direction, distribution, decay rate, etc.), then the PPF will be swamped by the BPF. The coupling system between a plane EMW and the static magnetic field is just this case (see Fig. 2), which will have the same or very similar sensitivity as the inverse G effect. We assume the power of the background EMW is 10 W, and it is limited in the cross section of $\Delta s = 0.1 \times 0.1 = 0.01 \text{ m}^2$. Because the power flux of the plane EMW is distributed homogeneously in the cross section Δs, then

$$\langle P_{em} \rangle = \text{Re}\left(\frac{1}{2\mu_0} E_x^{*(0)} B_y^{(0)}\right)\Delta s = \frac{1}{2\mu_0}\frac{E_x^{(0)2}}{c}\Delta s = 10 \text{ W}$$
$$\text{and} \quad |\vec{E}_x^{(0)}| \approx 8.7 \times 10^2 \text{ V m}^{-1}. \quad (14)$$
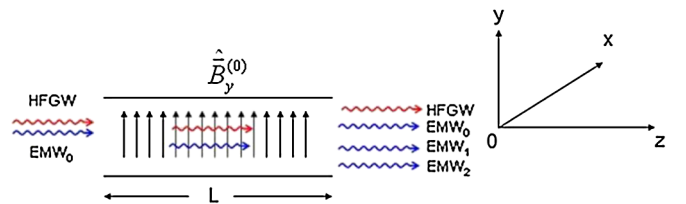

FIG. 2 (color online). If the HFGW and the EMW_0 pass simultaneously through the transverse static magnetic field, under the resonant state ($\omega_e = \omega_g$), the first-order perturbative EMW (EMW_1, i.e., "the interference term") and the second-order perturbative EMW (EMW_2) can be generated. However, because the EMW_1 and the EMW_0 have the same propagating direction and distribution, and EMW_1 is often much less than the EMW_0, the EMW_1 will be swamped by the EMW_0.

The total background photon flux passing through the cross section Δs will be

$$N_\gamma^{(0)} = 10/\hbar\omega_e = \frac{10}{3.3 \times 10^{-24}} \approx 3.0 \times 10^{24} \text{ s}^{-1}. \quad (15)$$

Then the corresponding first-order perturbative power flux in the z direction is

$$
\begin{aligned}
U_z^{(1)} &= \frac{1}{2\mu_0}[(\vec{E}^{(1)} \times \vec{B}_y^{(0)}) + (\vec{E}_x^{(0)} \times \vec{B}^{(1)})]_{\omega_e=\omega_g}\Delta s \\
&= \text{Re}\left[\frac{1}{\mu_0}E^{(1)*}B_y^{(0)}\right]\cos\beta\cos\delta \cdot \Delta s \\
&= \text{Re}\left[\frac{1}{\mu_0 c}E^{(1)*}E_x^{(0)}\right]\cos\beta\cos\delta \cdot \Delta s \\
&= \frac{1}{\mu_0 c}|\vec{E}^{(1)}||\vec{E}_x^{(0)}|\cos\beta\cos\delta \cdot \Delta s, \quad (16)
\end{aligned}
$$

where δ is the phase difference between the HFGW and the background EMW_0 and β is the angle between $\vec{E}^{(1)}$ and $\vec{E}_x^{(0)}$ or $\vec{B}^{(1)}$ and $\vec{B}_y^{(0)}$ (see Fig. 3). Here $\delta = 0$ and $\beta = 0$ will always be possible by regulating the phase and the polarization directions of the background EMW_0. Then the HFGW and the EMW will have the best matching state, i.e.,

$$
\begin{aligned}
U_z^{(1)}|_{\delta=0 \atop z=L} = U_{z\,\text{max}}^{(1)} &= \text{Re}\left[\frac{1}{\mu_0 c}E^{(1)*}E_x^{(0)}\right]\Delta s \\
&\approx 6.9 \times 10^{-20} \text{ W}. \quad (17)
\end{aligned}
$$

Then the corresponding first-order PPF will be

$$
\begin{aligned}
N_z^{(1)} = U_z^{(1)}/\hbar\omega_e &\approx 6.9 \times 10^{-20}/3.3 \times 10^{-24} \\
&\approx 2.1 \times 10^4 \text{ s}^{-1}. \quad (18)
\end{aligned}
$$

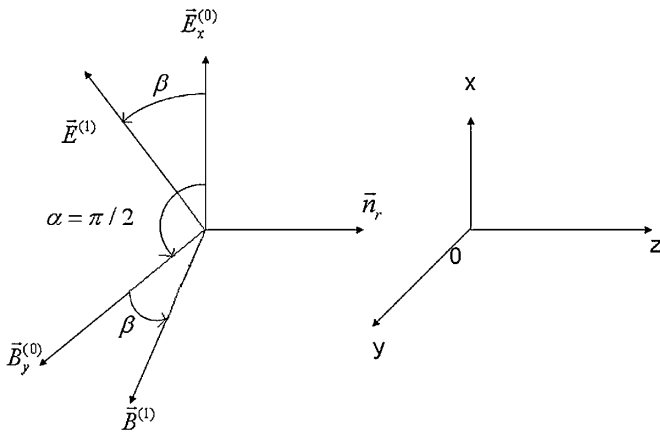Thus the total photon flux passing through Δs is about

FIG. 3. In the coupling system of the static magnetic field and the plane EMW, $|\vec{E}_x^{(0)}|$ and $|\vec{B}_y^{(0)}|$ denote the background EM fields, $|\vec{E}^{(1)}|$ and $|\vec{B}^{(1)}|$ express the perturbative EM fields generated by the direct interaction of the HFGW with the static magnetic field, and $\vec{n}_\gamma$ is the total photon flux density.

$$
\begin{aligned}
N_z &= N_z^{(0)} + N_z^{(1)} + N_z^{(2)} \\
&\approx (3.0 \times 10^{24} + 2.1 \times 10^4 + 7.0 \times 10^{-17}) \text{ s}^{-1}. \quad (19)
\end{aligned}
$$

In this case the ratio of $N_z^{(1)}$ and $N_z^{(0)}$ is roughly

$$\sigma_1 = N_z^{(1)}/N_z^{(0)} \approx \frac{2.1 \times 10^4}{3.0 \times 10^{24}} \approx 7.0 \times 10^{-21}. \quad (20)$$

This is also a very small value, and at the same time

$$\sigma_2 = N_z^{(2)}/N_z^{(1)} \approx \frac{7.0 \times 10^{-17}}{2.1 \times 10^4} \approx 3.3 \times 10^{-21}, \quad (21)$$

i.e., the second-order PPF is much less than the first-order PPF, while the first-order PPF is much less than the BPF. This means that if an EM detecting system contains simultaneously the static magnetic field and the EMW, then the interaction cross section between the GW (gravitons) and the EMW (photons) will be much larger than that in the pure inverse G effect. The classical description and linear quantum theory for such a property have good self-consistency [33,39].

However, Eqs. (3), (4), (14), (16), and (18) show that the first-order PPF (signal) and the BPF (noise) have the same propagating direction and distribution, and the BPF is much larger than the PPF, so that the PPF will be swamped by the BPF. In this case the PPF has no direct observable effect. According to Eqs. (3), (4), (17), and (18), one finds

$$
\begin{aligned}
&\text{if } \hat{h} = 10^{-26}/\sqrt{\text{Hz}}, \quad \text{then } N_z^{(1)} \approx 2.1 \times 10^8 \text{ s}^{-1}, \\
&\text{if } \hat{h} = 10^{-25}/\sqrt{\text{Hz}}, \quad \text{then } N_z^{(1)} \approx 2.1 \times 10^9 \text{ s}^{-1}.
\end{aligned}
\quad (22)
$$

For example, if $\hat{h} = 10^{-26}/\sqrt{\text{Hz}}$, in order to display first-order PPF, $N_z^{(1)}\Delta t$ must be effectively larger than the background noise fluctuation $\sqrt{N_z^{(0)}\Delta t}$, i.e.,

$$N_z^{(1)}(\Delta t)^{1/2} > \sqrt{N_z^{(0)}}, \quad \text{then } \Delta t > 6.8 \times 10^7 \text{ s}, \quad (23)$$

where $N_z^{(0)}\Delta t$ is the expectation value with a Poisson distribution of width $\sqrt{N_z^{(0)}}$. Equations (13) and (23) show that two such schemes have similar detecting sensitivity. Thus, detecting the HFGW of $\hat{h} = 10^{-26}/\sqrt{\text{Hz}}$ and $\nu = 5$ GHz by such a coupling EM system will also be very difficult.

IV. COUPLING SYSTEM OF THE STATIC MAGNETIC FIELD AND THE GAUSSIAN-TYPE MICROWAVE PHOTON FLUX

The above discussion shows that, in order to detect the first-order PPF, one must find a special EM resonant system in which the PPF and the BPF have very different physical behaviors, even if such differences are distributed only in a few local regions.

Before we discuss the resonance effect of the HFGWs in the proposal EM system, we give a general analysis of the

photon flux. Here $\vec{E}^{(0)}$ and $\vec{B}^{(0)}$ denote the background EM fields and $\vec{E}^{(1)}$ and $\vec{B}^{(1)}$ the perturbative EM fields produced by the interaction of the HFGW with the static magnetic field. Then total EM power flux density is

$$
\begin{aligned}
\vec{u}_{\rm em} &= \frac{1}{\mu_0}\vec{E}\times\vec{B} = \frac{1}{\mu_0}(\vec{E}^{(0)}+\vec{E}^{(1)})\times(\vec{B}^{(0)}+\vec{B}^{(1)}) \\
&= \frac{1}{\mu_0}\vec{E}^{(0)}\times\vec{B}^{(0)} + \frac{1}{\mu_0}(\vec{E}^{(0)}\times\vec{B}^{(1)}+\vec{E}^{(1)}\times\vec{B}^{(0)}) \\
&\quad + \frac{1}{\mu_0}\vec{E}^{(1)}\times\vec{B}^{(1)}.
\end{aligned}
\tag{24}
$$

Thus, the corresponding total photon flux density will be

$$
\begin{aligned}
\vec{n}_\gamma &= \frac{1}{\hbar\omega_e}\vec{u}_{\rm em} = \frac{1}{\mu_0\hbar\omega_e}(\vec{E}^{(0)}\times\vec{B}^{(0)}) \\
&\quad + \frac{1}{\mu_0\hbar\omega_e}(\vec{E}^{(0)}\times\vec{B}^{(1)}+\vec{E}^{(1)}\times\vec{B}^{(0)}) \\
&\quad + \frac{1}{\mu_0\hbar\omega_e}(\vec{E}^{(1)}\times\vec{B}^{(1)}) = \vec{n}^{(0)}+\vec{n}^{(1)}+\vec{n}^{(2)},
\end{aligned}
\tag{25}
$$

where

$$
\begin{aligned}
\vec{n}^{(0)} &= \frac{1}{\mu_0\hbar\omega_e}(\vec{E}^{(0)}\times\vec{B}^{(0)}), \\
\vec{n}^{(1)} &= \frac{1}{\mu_0\hbar\omega_e}(\vec{E}^{(0)}\times\vec{B}^{(1)}+\vec{E}^{(1)}\times\vec{B}^{(0)}), \\
\vec{n}^{(2)} &= \frac{1}{\mu_0\hbar\omega_e}(\vec{E}^{(1)}\times\vec{B}^{(1)}).
\end{aligned}
\tag{26}
$$

Equations (25) and (26) would be the most general form of the PPF and the BPF, where $\vec{n}^{(0)}$, $\vec{n}^{(1)}$, and $\vec{n}^{(2)}$ express the BPF, the first-order PPF, and the second-order PPF densities, respectively. Since nonvanishing $|\vec{E}^{(0)}|$ and $|\vec{B}^{(0)}|$ are often much larger than $|\vec{E}^{(1)}|$ and $|\vec{B}^{(1)}|$, we have

$$
|\vec{n}^{(0)}| \gg |\vec{n}^{(1)}| \gg |\vec{n}^{(2)}|.
\tag{27}
$$

A. In the case of the the plane EMW

If the HFGW and the plane EMW$_0$ all propagate along the z direction, then Eq. (25) is deduced to (see Fig. 3)

$$
\begin{aligned}
n_\gamma &= \langle\vec{n}_\gamma\rangle_{\omega_e=\omega_g} \\
&= \frac{1}{2\mu_0\hbar\omega_e}\langle(\vec{E}_x^{(0)}+\vec{E}^{(1)})\times(\vec{B}_y^{(0)}+\vec{B}^{(1)})\rangle_{\omega_e=\omega_g} \\
&= \frac{1}{2\mu_0\hbar\omega_e}\Big\{|\vec{E}_x^{(0)}||\vec{B}_y^{(0)}| + \Big[|\vec{E}_x^{(0)}||\vec{B}^{(1)}|\sin\Big(\frac{\pi}{2}+\beta\Big) \\
&\quad + |\vec{E}^{(1)}||\vec{B}_y^{(0)}|\sin\Big(\frac{\pi}{2}-\beta\Big)\Big]\cos\delta + |\vec{E}^{(1)}||\vec{B}^{(1)}|\Big\},
\end{aligned}
\tag{28}
$$

where the angular bracket denotes the average over time. For the plane EMW in empty space, $B_y^{(0)}=E_x^{(0)}/c$, $B^{(1)}=E^{(1)}/c$ (in mks units), then Eq. (28) becomes

$$
\begin{aligned}
n_\gamma &= \frac{1}{2\mu_0 c\hbar\omega_e}\{|\vec{E}_x^{(0)}|^2 + 2|\vec{E}_x^{(0)}||\vec{E}^{(1)}|\cos\beta\cos\delta + |\vec{E}^{(1)}|^2\} \\
&= \frac{1}{2\mu_0 c\hbar\omega_e}\{|\vec{E}_x^{(0)}|^2 + 2\vec{E}_x^{(0)}\cdot\vec{E}^{(1)}\cos\delta + |\vec{E}^{(1)}|^2\} \\
&= n^{(0)}+n^{(1)}+n^{(2)},
\end{aligned}
\tag{29}
$$

where

$$
\begin{aligned}
n^{(0)} &= \frac{1}{2\mu_0 c\hbar\omega_e}|\vec{E}_x^{(0)}|^2, \\
n^{(1)} &= \frac{1}{\mu_0 c\hbar\omega_e}\vec{E}_x^{(0)}\cdot\vec{E}^{(1)}\cos\delta, \\
n^{(2)} &= \frac{1}{2\mu_0 c\hbar\omega_e}|\vec{E}^{(1)}|^2.
\end{aligned}
\tag{30}
$$

In fact, Eq. (30) can also be expressed as

$$
\begin{aligned}
n^{(0)} &= \frac{1}{2\mu_0 c\hbar\omega_e}|\vec{E}_x^{(0)}|^2 \\
&= \dot{N}_0 \text{ (the background photon flux density)}, \\
n^{(2)} &= \frac{1}{2\mu_0 c\hbar\omega_e}|\vec{E}^{(1)}|^2 \\
&= \dot{N}_{\rm GW} \text{ (the second-order PPF density)},
\end{aligned}
\tag{31}
$$

while

$$
n^{(1)} = \frac{1}{\mu_0 c\hbar\omega_e}\vec{E}_x^{(0)}\cdot\vec{E}^{(1)}\cos\delta = 2(\dot{N}_0\dot{N}_{\rm GW})^{1/2}\cos\delta = \dot{N}_1 \text{ (the interference term, i.e., the first-order PPF density).}
\tag{32}
$$

Then, Eq. (29) can be rewritten as

$$
n_\gamma = \dot{N}_0 + 2(\dot{N}_0\dot{N}_{\rm GW})^{1/2}\cos\delta + \dot{N}_{\rm GW}.
\tag{33}
$$

After a long time interval Δt, the collected number of photons at the detector or at the receiving surface would be

$$
\begin{aligned}
N_d &= n_\gamma\Delta t \\
&= \dot{N}_0\Delta t + 2(\dot{N}_0\dot{N}_{\rm GW})^{1/2}\cos\delta\cdot\Delta t + \dot{N}_{\rm GW}\Delta t.
\end{aligned}
\tag{34}
$$

Clearly, in the plane EMW case, the BPF, the first-order PPF, and the second-order PPF all propagate along the same direction; thus in any region and at any receiving surface

$$
\dot{N}_0 \gg 2(\dot{N}_0\dot{N}_{\rm GW})^{1/2} \gg \dot{N}_{\rm GW}
\tag{35}
$$

is always valid. In this case, it is very difficult to display the first-order PPF effect $[n^{(1)}=2(\dot{N}_0\dot{N}_{\rm GW})^{1/2}\cos\delta=\dot{N}_1]$ in
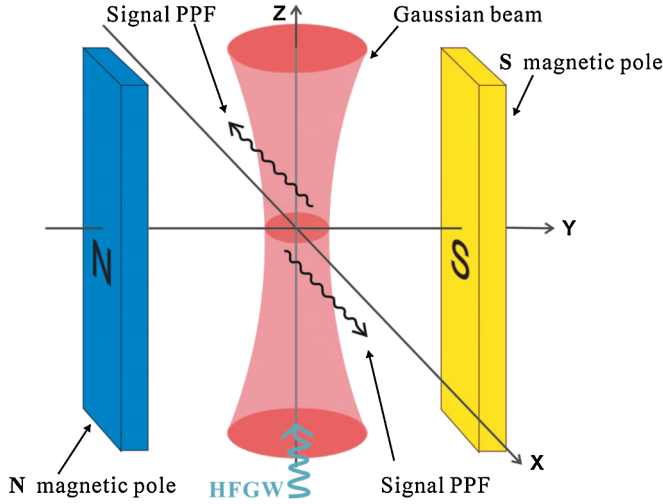
FIG. 4 (color online).   When the HFGW propagates along the z direction in the coupling system of the GB and the transverse static magnetic field $\hat{\vec{B}}_y^{(0)}$, the resonant interaction ($\omega_e = \omega_g$) of the HFGW with the EM fields will generate not only the longitudinal perturbative photon flux $n_z^{(1)}$ but also the transverse perturbative photon fluxes ($n_x^{(1)}$ and $n_y^{(1)}$) in the x and y directions due to the spread property of the GB itself. This is an important difference between Figs. 2 and 4. Moreover, unlike $n_z^{(1)}$ and $n_z^{(0)}$, $n_x^{(1)}$ and $n_x^{(0)}$ have very different distribution and decay rates.

an acceptable signal accumulation time interval with the predicted total photon flux background.

In the coupling system between the Gaussian-type microwave photon flux [the Gaussian beam (GB) is just one typical form of the Gaussian-type microwave photon fluxes] and the static magnetic field, the general expressions Eqs. (25) and (26) are still valid. However, they will be expressed as the different exact forms in the different directions and the receiving surfaces, and the relative relation between $n^{(0)}$ and $n^{(1)}$ would be different in the different receiving surfaces; even then they can reach up to a comparable order of magnitude. This is worth consideration. The scheme from [32] would be a useful candidate (see Fig. 4). Thus key parameters in the scheme are the BPF and the first-order PPF in the special directions and not the photon number. The former are vectors and have high directivity. They decide the strength of the photon fluxes reaching the detector or the receiving surface, position, and bearings of the detectors and the signal-to-noise ratio (SNR) in the receiving surfaces.

B. Coupling system of the Gaussian-type microwave photon flux and the static magnetic field

Unlike the plane EMW, the GB has not only the longitudinal BPF (the BPF in the z direction, i.e., the direction of its symmetrical axis) but also the transverse BPF, although the latter is often less than the former. The BPF in the transverse directions (e.g., the x and y directions) decays as

fast as the typical Gaussian decay rate. Thus, in the some special regions and directions, the effect of both the PPF and the BPF would have a comparable order of magnitude.

For the GB with the double transverse polarized electric modes [32,40], it has

$$\vec{E}^{(0)} = \vec{E}_x^{(0)} + \vec{E}_y^{(0)}, \qquad \vec{B}^{(0)} = \vec{B}_x^{(0)} + \vec{B}_y^{(0)} + \vec{B}_z^{(0)}. \quad (36)$$

Such EM fields satisfy the Helmholtz equation. If the circular polarized HFGW propagates along the z direction, then the nonvanishing perturbative EM fields are $\vec{E}_x^{(1)}$, $\vec{B}_y^{(1)}$ (the perturbative EM fields produced by the $\oplus$ polarization component of the HFGW) and $\vec{E}_y^{(1)}$, $\vec{B}_x^{(1)}$ (the perturbative EM fields generated by the $\otimes$ polarization component of the HFGW) in our scheme [32]], respectively, i.e.,

$$\vec{E}^{(1)} = \vec{E}_x^{(1)} + \vec{E}_y^{(1)}, \qquad \vec{B}^{(1)} = \vec{B}_x^{(1)} + \vec{B}_y^{(1)}. \quad (37)$$

In this case, Eq. (25) has following concrete expression:

$$\vec{n}_\gamma = \frac{1}{\mu_0 \hbar \omega_e} \vec{E} \times \vec{B} = \frac{1}{\mu_0 \hbar \omega_e} \{(\vec{E}_x^{(0)} + \vec{E}_x^{(1)} + \vec{E}_y^{(0)} + \vec{E}_y^{(1)})$$
$$\times (\vec{B}_x^{(0)} + \vec{B}_x^{(1)} + \vec{B}_y^{(0)} + \vec{B}_y^{(1)} + \vec{B}_z^{(0)})\}. \quad (38)$$

From Eq. (38), under the resonant state ($\omega_e = \omega_g$) the total photon flux densities in the z direction (the longitudinal direction of the GB) and in the transverse direction (the x and y directions) can be given by

$$n_z = \frac{1}{2\mu_0 \hbar \omega_e} \mathrm{Re}\{[E_x^{*(0)} B_y^{(0)} + E_y^{*(0)} B_x^{(0)}]$$
$$+ [E_x^{*(0)} B_y^{(1)} + E_y^{*(0)} B_x^{(1)} + E_x^{*(1)} B_y^{(0)} + E_y^{*(1)} B_x^{(0)}]$$
$$+ [E_x^{*(1)} B_y^{(1)} + E_y^{*(1)} B_x^{(1)}]\}$$
$$= n_z^{(0)} + n_z^{(1)} + n_z^{(2)} = n_z^{(0)} + n_z^{(1)} + o(h^2), \quad (39)$$

$$n_x = \frac{1}{2\mu_0 \hbar \omega_e} \mathrm{Re}[E_y^{*(0)} B_z^{(0)} + E_y^{*(1)} B_z^{(0)}] = n_x^{(0)} + n_x^{(1)}, \quad (40)$$

$$n_y = \frac{1}{2\mu_0 \hbar \omega_e} \mathrm{Re}[E_x^{*(0)} B_z^{(0)} + E_x^{*(1)} B_z^{(0)}] = n_y^{(0)} + n_y^{(1)}. \quad (41)$$

The photon flux in the z direction (the longitudinal direction of the GB).—From Eq. (39) and Refs. [32,40], we have

$$n_z^{(0)} = |n_z^{(0)}|_{\max} \exp\left(-\frac{2r^2}{W^2}\right),$$
$$n_z^{(1)} = |n_z^{(1)}|_{\max} \exp\left(-\frac{r^2}{W^2}\right), \quad (42)$$

where r is the radial distance to the symmetrical axis (the z axis) of the GB and W is the spot radius of the GB. Equation (42) shows that $n_z^{(0)}$ decays by the typical
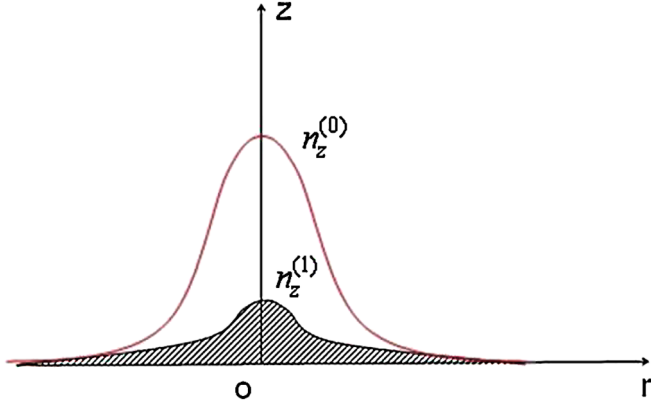
FIG. 5 (color online). The first-order PPF density $n_z^{(1)}$ and the BPF density $n_z^{(0)}$ have the same propagating direction and similar distribution. Thus $n_z^{(0)}$ is much larger than $n_z^{(1)}$ in most of the regions.

Gaussian decay rate $\exp(-\frac{2r^2}{W^2})$, while $n_z^{(1)}$ decays by the factor $\exp(-\frac{r^2}{W^2})$; i.e., the decay rate of $n_z^{(1)}$ is slower than that of $n_z^{(0)}$. However, since $|n_z^{(0)}|_{\max} \gg |n_z^{(1)}|_{\max}$ in almost all of the regions (see Fig. 5), it is difficult to generate an observable effect by $n_z^{(1)}$ in these regions. For the HFGW parameters of $h = 10^{-30}/\sqrt{\text{Hz}}$ and $\nu = 5$ GHz, only if $r \rightarrow 34$ cm (at the xy plane), $n_z^{(1)}$ has a comparable order of magnitude with $n_z^{(0)}$. However, $n_z^{(1)}$ and $n_z^{(0)}$ all are decayed to the very small undetectable value $n_z^{(1)} \sim n_z^{(0)} \sim 10^{-16}$ s^{-1} m^{-2}.

The photon fluxes in the x direction (the transverse direction of the GB).—According to Eq. (40) and Refs. [32,40], one finds

$$n_x = \frac{1}{2\mu_0 \hbar \omega_e} \langle |\vec{E}_y^{(0)}||\vec{B}_z^{(0)}| + |\vec{E}_y^{(1)}||\vec{B}_z^{(0)}| \cos\delta \rangle_{\omega_e = \omega_g}. \tag{43}$$

Setting $\delta = 0$ will always be possible by regulating the phase of the GB. Then

$$n_x = \frac{1}{2\mu_0 \hbar \omega_e} \{ \langle \vec{E}_y^{(0)} \vec{B}_z^{(0)} \rangle + \langle \vec{E}_y^{(1)} \vec{B}_z^{(0)} \rangle \}_{\omega_e = \omega_g}$$
$$= n_x^{(0)} + n_x^{(1)} = \dot{N}_{0x} + \dot{N}_{1x}, \tag{44}$$

where

$$n_x^{(0)} = \dot{N}_{0x} = \frac{1}{2\mu_0 \hbar \omega_e} \langle |\vec{E}_y^{(0)}||\vec{B}_z^{(0)}| \rangle$$
$$= |n_x^{(0)}|_{\max} x \exp\left(-\frac{2x^2}{W^2}\right), \tag{45}$$

$$n_x^{(1)} = \dot{N}_{1x} = \frac{1}{2\mu_0 \hbar \omega_e} \langle |\vec{E}_y^{(1)}||\vec{B}_z^{(0)}| \rangle_{\omega_e = \omega_g}$$
$$= |n_x^{(1)}|_{\max} \exp\left(-\frac{x^2}{W^2}\right). \tag{46}$$

Unlike the case of the plane EMW, Eqs. (45) and (46) show that $\dot{N}_{0x}$ will be not always larger than $\dot{N}_{1x}$. In the case of the GB, $B_z^{(0)}$ of the GB depends on not only $\vec{E}_y^{(0)}$, but also $\vec{E}_x^{(0)}$, i.e.,

$$B_z^{(0)} = \frac{i}{\omega_e}\left(\frac{\partial E_x^{(0)}}{\partial y} - \frac{\partial E_y^{(0)}}{\partial x}\right). \tag{47}$$

Therefore, when $E_y^{(0)} = 0$, $n_x^{(0)}$ must be vanish, but $n_x^{(1)} = n_{x\max}^{(1)} \neq 0$.

Although Eqs. (45) and (46) represent the transverse photon fluxes in the x direction, their physical behaviors are quite different:

(1) At the yz plane, $n_x^{(1)}|_{x=0} = n_x^{(1)}|_{\max}$, where $n_x^{(0)}|_{x=0} = 0$; i.e., the transverse PPF has a maximum at the longitudinal symmetrical surface of the GB where the transverse BPF vanishes (see Fig. 6). It should be pointed out that the transverse BPF at the longitudinal symmetrical surfaces being identically to zero is a fundamental characteristic of the GBs, whether the circular or elliptic GBs. Thus the transverse PPF would be a major fraction of the total transverse photon fluxes flux passing through such a surface, provided the other noise photon flux passing through the surface can be effectively suppressed, although the PPF is much less than the BPF in other regions, and the PPF is always accompanied simultaneously by the BPF.

(2) The $n_x^{(1)}$ and $n_x^{(0)}$ have different decay rates in the x direction, i.e., $n_x^{(1)} \propto \exp(-\frac{x^2}{W^2})$ and $n_x^{(0)} \propto x \exp(-\frac{2x^2}{W^2})$, respectively. The position of a maximum of $n_x^{(1)}$ is the yz plane ($x = 0$), while the position of a maximum of $n_x^{(0)}$ is about $x = 3.2$ cm in our case. Thus, the SNR $n_x^{(1)}/n_x^{(0)}$ will be very different at the different receiving surfaces. This means that it is always possible to obtain a best SNR $n_x^{(1)}/n_x^{(0)}$ by choosing the suitable region and the receiving surface. Using Eqs. (45) and (46), the total transverse photon fluxes passing through the receiving surface Δs can be given by

$$N_x^{(1)} = \int_{\Delta s} n_x^{(1)} ds, \tag{48}$$

$$N_x^{(0)} = \int_{\Delta s} n_x^{(0)} ds. \tag{49}$$

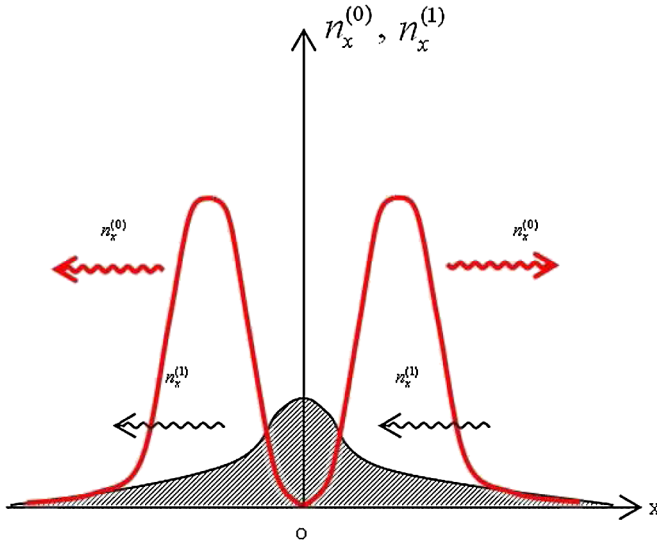In the current scheme, $\Delta s \approx 10^{-2}$ m^2.

FIG. 6 (color online). Schematic diagram of strength distribution of $n_x^{(0)}$ and $n_x^{(1)}$ in the "outgoing wave" region of the GB (another one is the "imploding wave" region. For an optimum GB, such properties of the transverse BPFs in two such regions would be "antisymmetric"). Unlike Fig. 5, here $n_x^{(0)}|_{x=0} = 0$ while $n_x^{(1)}|_{x=0} = n_x^{(1)}|_{\max}$. Therefore, $n_x^{(1)}\Delta t$ can be effectively larger than the background noise photon flux fluctuation $(n_x^{(0)}\Delta t)^{1/2}$; i.e., $n_x^{(1)}\Delta t > (n_x^{(0)}\Delta t)^{1/2}$ at the yz plane and at the parallel surfaces near the yz plane, and $n_x^{(1)}$ will be a major fraction of the total transverse photon flux passing through the yz plane, provided thermal photon flux and other noise photon fluxes passing through the surface can be effectively suppressed. Clearly, the EM response of the coupling system between the plane EMW and the static magnetic field has no such characteristic. Moreover, the propagating directions of $n_x^{(1)}$ are opposite in the regions of $y > 0$ and $y < 0$ for our scheme. Thus, the total momentum of the PPF in the x direction vanishes. In other words, such a property ensured conservation of the total momentum in the coherent resonance interaction (see Ref. [32]).

C. Numerical estimation of the transverse photon fluxes

In order to measure $N_x^{(1)}$ at a suitable receiving surface, $N_x^{(1)}\Delta t$ [notice that here $N_x^{(1)}$ is equivalent to $2(\dot{N}_0\dot{N}_{GW})^{1/2}$ in the plane EMW case, but $N_x^{(1)}$ in our case and $2(\dot{N}_0\dot{N}_{gw})^{1/2}$ in the plane EM case have a very different physical behavior] must be effectively larger than the noise photon fluctuation $(N_x^{(0)}\Delta t)^{1/2}$, i.e.,

$$N_x^{(1)}\Delta t > (N_x^{(0)}\Delta t)^{1/2}, \tag{50}$$

then

$$\Delta t > \frac{N_x^{(0)}}{(N_x^{(1)})^2} = \Delta t_{\min}, \tag{51}$$

where $\Delta t_{\min}$ is requisite minimal signal accumulation time at the noise background $N_x^{(0)}$. In fact, Eqs. (50) and (51) are the exact forms from the general relation equations (25)

and (26), while Eq. (23) is the exact form from the general relation equations (25) and (26) in the plane EMW case. In the following, we list the $N_x^{(1)}$, $N_x^{(0)}$, $\Delta t_{\min}$, and measurable HFGW strength h_{rms} at the different receiving surfaces. If $x = 0$ (the yz plane), then $N_x^{(0)} = 0$; it would be best measuring in the region for $N_x^{(1)}$. Of course, this does not mean that there are no other noise photon fluxes passing through the receiving surface Δs. In fact, scattering, diffraction, and drift of the BPF and the thermal noise caused by the BPF all can generate smaller noise photon fluxes passing through the surface Δs. Since they are all caused by the BPF, they should have the same decay factor $\exp(-\frac{2x^2}{W^2})$ as the BPF. Moreover, external EM noise and the thermal noise caused by the environmental temperature are independent of the BPF, but they can be effectively suppressed by high-quality Faraday cage or shielding covers and low-temperature ($T \sim 1$ K or less) vacuum operation. In general, they are much less than the BPF. Issues such as the thermal noise, the radiation press noise, and the noise caused by the scattering for this scheme have been discussed in Ref. [41], so we shall not repeat them here. Thus, our attention will be focused only on the BPF itself and the other noise photon flux $N_{x(\mathrm{other})}^{(0)}$ caused by the BPF. In this case, if such noise photon fluxes passing through the receiving surface Δs at the yz plane can be limited to a realizable level, then we can estimate the minimal signal accumulation time $\Delta t_{\min}$ in the noise background.

From the above discussion, Eqs. (48) and (49), and Ref. [32,40], the signal photon flux $N_x^{(1)}$ and the background photon flux $N_x^{(0)}$ passing through Δs are

$$N_x^{(1)} = |N_x^{(1)}|_{\max} \exp\left(-\frac{x^2}{W^2}\right), \tag{52}$$

$$N_x^{(0)} = |N_x^{(0)}|_{\max} x \exp\left(-\frac{2x^2}{W^2}\right), \tag{53}$$

and

$$N_{x(\mathrm{other})}^{(0)} = |N_{x(\mathrm{other})}^{(0)}|_{\max} \exp\left(-\frac{2x^2}{W^2}\right). \tag{54}$$

The displaying condition in the receiving surfaces will be

$$N_x^{(1)}(\Delta t)^{1/2} \geq [N_x^{(0)} + N_{x(\mathrm{other})}^{(0)}]^{1/2}, \tag{55}$$

and thus

$$\Delta t \geq \frac{x|N_x^{(0)}|_{\max} + |N_{x(\mathrm{other})}^{(0)}|_{\max}}{|N_x^{(1)}|_{\max}^2} \quad \text{and}$$

$$\Delta t_{\min} = \frac{x|N_x^{(0)}|_{\max} + |N_{x(\mathrm{other})}^{(0)}|_{\max}}{|N_x^{(1)}|_{\max}^2}, \tag{56}$$

where $|N_x^{(0)}|_{\max} \approx 1.2 \times 10^{22}$ s^{-1} in the typical parameter condition of the scheme.

Considering a possible laboratory condition, we choose the typical parameters in Ref. [32], i.e., $\hat{B}_y^{(0)} = 3$ T, $L = 6$ m, and $P = 10$ W. Then we can estimate $\Delta t_{\min}$ in the different HFGW parameter conditions.

(1) $x = 0$, then $N_x^{(0)} \equiv 0$, *from Eqs.* (53) *and* (56).—

$$\Delta t_{\min} = \frac{|N_{x(\text{other})}^{(0)}|_{\max}}{|N_x^{(1)}|_{\max}^2}. \tag{57}$$

If $\hat{h} = 10^{-30}/\sqrt{\text{Hz}}$, then

$$N_x^{(1)} = |N_x^{(1)}|_{\max} \approx 8.2 \times 10^2 \text{ s}^{-1} \quad \text{and}$$

$$\Delta t_{\min} \approx 3.0 \times 10^3 \text{ s provided}$$

$$|N_{x(\text{other})}^{(0)}|_{\max} < 2.1 \times 10^9 \text{ s}^{-1},$$

$$\Delta t_{\min} \approx 3.0 \times 10^5 \text{ s} \sim 3.5 \text{ days provided}$$

$$|N_{x(\text{other})}^{(0)}|_{\max} < 2.1 \times 10^{11} \text{ s}^{-1} \ (\sim 0.7 \text{ PW}). \tag{58}$$

If $\hat{h} = 10^{-27}/\sqrt{\text{Hz}}$, then

$$|N_x^{(1)}|_{\max} \approx 8.2 \times 10^5 \text{ s}^{-1}$$

and $\quad \Delta t_{\min} \approx 3.0 \times 10^3 \text{ s provided}$

$$|N_{x(\text{other})}^{(0)}|_{\max} < 2.1 \times 10^{15} \text{ s}^{-1},$$

$$\Delta t_{\min} \approx 3.0 \times 10^5 \text{ s} \sim 3.5 \text{ days provided}$$

$$|N_{x(\text{other})}^{(0)}|_{\max} < 2.1 \times 10^{17} \text{ s}^{-1}. \tag{59}$$

If $\hat{h} = 10^{-26}/\sqrt{\text{Hz}}$, then

$$|N_x^{(1)}|_{\max} \approx 8.2 \times 10^6 \text{ s}^{-1} \quad \text{and}$$

$$\Delta t_{\min} \approx 3.0 \times 10^3 \text{ s provided}$$

$$|N_{x(\text{other})}^{(0)}|_{\max} < 2.1 \times 10^{17} \text{ s}^{-1},$$

$$\Delta t_{\min} \approx 3.0 \times 10^5 \text{ s} \sim 3.5 \text{ days provided}$$

$$N_{x(\text{other})}^{(0)} < 2.1 \times 10^{19} \text{ s}^{-1}. \tag{60}$$

If $\hat{h} = 10^{-24}/\sqrt{\text{Hz}}$, then

$$|N_x^{(1)}|_{\max} \approx 8.2 \times 10^8 \text{ s}^{-1} \quad \text{and}$$

$$\Delta t_{\min} \approx 3.0 \times 10^3 \text{ s provided}$$

$$|N_{x(\text{other})}^{(0)}|_{\max} < 2.1 \times 10^{21} \text{ s}^{-1},$$

$$\Delta t_{\min} \approx 3.0 \times 10^5 \text{ s} \sim 3.5 \text{ days provided}$$

$$|N_{x(\text{other})}^{(0)}|_{\max} < 2.1 \times 10^{23} \text{ s}^{-1}. \tag{61}$$

The above results show that limitation to the other noise photon fluxes passing through Δs would be very relaxed. It is interesting to compare the scheme employed earlier [see Eq. (23), where $\hat{h} = 10^{-26}/\sqrt{\text{Hz}}$, $\nu = 5$ GHz, $\hat{B}_y^{(0)} = 10$ T, $L = 10$ m, and $P = 10$ W] and the current scheme [see Eq. (60), where $\hat{h} = 10^{-26}/\sqrt{\text{Hz}}$, $\nu = 5$ GHz, $\hat{B}^{(0)} = 3$ T, $L = 6$ m, and $P = 10$ W]; they show that the current scheme has obvious advantages and reality.

(2) $x = 1$ cm $= 10^{-2}$ m, *then* $N_x^{(0)} \approx 1.1 \times 10^{20} \text{ s}^{-1}$, *but where* $|N_{x(\text{other})}^{(0)}|_{\max}$ *is often much less than* $N_x^{(0)}$; *i.e.,* $N_{x(\text{other})}^{(0)}$ *can be neglected in all of the following discussions.*—From Eq. (56), we have

$$
\begin{aligned}
\hat{h} = 10^{-26}/\sqrt{\text{Hz}}, &\quad N_x^{(1)} \approx 7.8 \times 10^6 \text{ s}^{-1}, &\quad \Delta t_{\min} \approx 1.8 \times 10^6 \text{ s};\\
\hat{h} = 10^{-25}/\sqrt{\text{Hz}}, &\quad N_x^{(1)} \approx 7.8 \times 10^7 \text{ s}^{-1}, &\quad \Delta t_{\min} \approx 1.8 \times 10^4 \text{ s};\\
\hat{h} = 10^{-24}/\sqrt{\text{Hz}}, &\quad N_x^{(1)} \approx 7.8 \times 10^8 \text{ s}^{-1}, &\quad \Delta t_{\min} \approx 1.8 \times 10^2 \text{ s}.
\end{aligned}
\tag{62}
$$

(3) $x = 2$ cm $= 2 \times 10^{-2}$ m, *then* $N_x^{(0)} \approx 1.7 \times 10^{20} \text{ s}^{-1}$.—

$$
\begin{aligned}
\hat{h} = 10^{-26}/\sqrt{\text{Hz}}, &\quad N_x^{(1)} \approx 7.0 \times 10^6 \text{ s}^{-1}, &\quad \Delta t_{\min} \approx 3.5 \times 10^6 \text{ s};\\
\hat{h} = 10^{-25}/\sqrt{\text{Hz}}, &\quad N_x^{(1)} \approx 7.0 \times 10^7 \text{ s}^{-1}, &\quad \Delta t_{\min} \approx 3.5 \times 10^4 \text{ s};\\
\hat{h} = 10^{-24}/\sqrt{\text{Hz}}, &\quad N_x^{(1)} \approx 7.0 \times 10^8 \text{ s}^{-1}, &\quad \Delta t_{\min} \approx 3.5 \times 10^2 \text{ s}.
\end{aligned}
\tag{63}
$$

(4) $x = 3$ cm $= 3 \times 10^{-2}$ m, *then* $N_x^{(0)} \approx 1.8 \times 10^{20} \text{ s}^{-1}$.—

$$\hat{h} = 10^{-26}/\sqrt{\text{Hz}}, \qquad N_x^{(1)} \approx 5.8 \times 10^6 \text{ s}^{-1}, \qquad \Delta t_{\min} \approx 5.4 \times 10^6 \text{ s};$$

$$\hat{h} = 10^{-25}/\sqrt{\text{Hz}}, \qquad N_x^{(1)} \approx 5.8 \times 10^7 \text{ s}^{-1}, \qquad \Delta t_{\min} \approx 5.4 \times 10^4 \text{ s}; \qquad (64)$$

$$\hat{h} = 10^{-24}/\sqrt{\text{Hz}}, \qquad N_x^{(1)} \approx 5.8 \times 10^8 \text{ s}^{-1}, \qquad \Delta t_{\min} \approx 5.4 \times 10^2 \text{ s}.$$

(5) $x = 10$ cm $= 0.1$ m, *then* $N_x^{(0)} \approx 4.0 \times 10^{17}$ s^{-1}.—

$$\hat{h} = 10^{-26}/\sqrt{\text{Hz}}, \qquad N_x^{(1)} \approx 1.5 \times 10^5 \text{ s}^{-1}, \qquad \Delta t_{\min} \approx 1.2 \times 10^7 \text{ s};$$

$$\hat{h} = 10^{-25}/\sqrt{\text{Hz}}, \qquad N_x^{(1)} \approx 1.5 \times 10^6 \text{ s}^{-1}, \qquad \Delta t_{\min} \approx 1.2 \times 10^5 \text{ s}; \qquad (65)$$

$$\hat{h} = 10^{-24}/\sqrt{\text{Hz}}, \qquad N_x^{(1)} \approx 1.5 \times 10^7 \text{ s}^{-1}, \qquad \Delta t_{\min} \approx 1.2 \times 10^3 \text{ s}.$$

(6) $x = 29$ cm *(about the distance of 6 spot radii of the GB)*, $\hat{h} = 10^{-26}/\sqrt{\text{Hz}}$, then $N_x^{(0)} \approx N_x^{(1)} \approx 2.1 \times 10^{-8}$ s^{-1}.—The time of receiving one transversal photon would be $\Delta t_{\min} \approx \frac{1}{N_x^{(0)}} \approx \frac{1}{N_x^{(1)}} \approx \frac{1}{2.1 \times 10^{-8} \text{ s}^{-1}} = 4.8 \times 10^7$ s.

The above numerical estimation shows:

(1) The best position for displaying $N_x^{(1)}$ would be in the yz plane and the other parallel receiving surfaces in the region of -2 cm $< x < 2$ cm. In such regions, the transverse PPF $N_x^{(1)}$ for the parameter condition $\hat{h} \sim 10^{-24}$–$10^{-30}/\sqrt{\text{Hz}}$ may reach up to $\sim 8.2 \times 10^8$ to 8.2×10^2 s^{-1}. If other noise photon fluxes passing through the surfaces can be effectively suppressed into $\sim 2.1 \times 10^{23}$ to $\sim 2.1 \times 10^9$ s^{-1}, then the corresponding minimal signal accumulation time $\Delta t_{\min}$ in the noise photon flux background would be $\sim 10^3$ to 10^5 s.

(2) Unlike $N_x^{(1)}$, $N_x^{(0)}$ has a maximum at $x \sim 3.2$ cm, where $N_x^{(0)} \gg N_x^{(1)}$, but $N_x^{(1)}|_{x=3.2 \text{ cm}}$ and $N_x^{(1)}|_{x=0} = N_x^{(1)}|_{\max}$ have the same order of magnitude. In the region, the detecting sensitivity would be worse by 3–4 orders of magnitude over that at the yz plane.

(3) Since $N_x^{(1)} = |N_x^{(1)}|_{\max} \exp(-\frac{x^2}{W^2})$ and $N_x^{(0)} = |N_x^{(0)}|_{\max} x \exp(-\frac{2x^2}{W^2})$, even if $\hat{h} = 10^{-26}/\sqrt{\text{Hz}}$, they will have the same order of magnitude in $x \approx 29$ cm. However, where $N_x^{(0)}$, $N_x^{(1)}$ all decay to 2.1×10^{-8} s^{-1}.

Moreover, it was shown that if the propagating detections of $N_x^{(0)}$ and $N_x^{(1)}$ are the same in the 1st, 3rd, 6th, and 8th octants in our case, then they will propagate along the opposite directions in the 2nd, 4th, 5th, and 7th octants [32]. This means the distinguishing ability to $N_x^{(0)}$ and $N_x^{(1)}$ of the scheme can be further improved. Also, as suggested by Baker [42], since the BPF is unaffected by the magnetic field (it is involved only in the generation of the PPF), one can differentiate the PPF from the BPF by modulating the magnetic field. This essentially eliminates the BPF by microwave-receiver signal processing. For example, one measures the BPF plus PPF with the magnet on and then measures the BPF alone with the magnet off and subtracts one from the other in order to obtain the PPF alone. This process is accomplished more rigorously by statistical signal processing.

D. Role of fractal membranes or other equivalent microwave lenses

(1) The fractal membranes (FMs) are merely one of many possible ways to improve the SNR and detecting quality via the redirection of signal photons onto the microwave detectors [32]. However, in the above discussion, the proposal scheme did not involve the FMs. In other words, even if we do not use the FMs, the above-mentioned relation between the PPF and the BPF is still valid. The fractal membranes in the gigahertz band have successfully been developed by the Hong Kong University of Science and Technology [43–45] from 2002 to 2005. First, the FMs have very good selection ability to the photon fluxes in the gigahertz band. If the FM is nearly totally reflecting for the photon fluxes with certain frequencies in the gigahertz band, then it will be nearly total transmitting for the photon fluxes with other frequencies in the gigahertz band. Second, the FMs have a good focus function to the photon fluxes in the gigahertz band. For example, the photon fluxes reflected and transmitted by the FMs can keep their strength invariant within the distance of 1 m from the FMs. Such a function has been proven by experimental tests. The role of the FMs in the scheme is only the reflector or the transmitter for the photon flux in the gigahertz band. Because $N_z^{(0)}$, $N_y^{(0)}$ and $N_x^{(0)}$, $N_x^{(1)}$ are exactly orthogonal for each other, an FM (or an equivalent microwave lens) parallel with the yz plane would focus only $N_x^{(0)}$, $N_x^{(1)}$ and not $N_z^{(0)}$, $N_y^{(0)}$. In fact, here the requirement for the FMs is also more relaxed; i.e., it does not require focusing

the photon flux onto a micron-sized detector even into a point. In the typical parameter condition of the scheme, if the cross section of the focusing photon flux and the image size has the same or close size in the detector (in a distance of ~28 cm), then the SNR $N_x^{(1)}/N_x^{(0)}$ at the receiving surface Δs and at the image surface $\Delta s'$ would be nearly the same. Moreover, because unfocused $N_z^{(0)}$, $N_y^{(0)}$ will be decayed to 10^{-7} s^{-1} at $x = 29$ cm, their influence can be neglected there.

(2) If the FM is just laid at the symmetrical plane (the yz plane) or at the parallel planes very near the yz plane (see Figs. 7 and 8), then the wave fronts of the photon fluxes passing through the receiving surfaces Δs at the planes would be the plane or the pseudo-plane, i.e., where it is possible to obtain a better focusing effect. The requirement for the focus in the region would be more relaxed than other regions. This is because such focusing quality depends only on the local interaction of the photon fluxes at the receiving surfaces in the region of $|x| \le 2$ cm. Besides, provided the photon fluxes focused by the FM can keep a plane or pseudoplane wave front, then $N_x^{(0)}$, $N_x^{(1)}$ focused simultaneously on another surface $\Delta s'$ would have the same or nearly the same SNR as with that at Δs. A unique requirement for $N_x^{(1)}$ and $N_x^{(0)}$ at $\Delta s'$ is that $N_x^{(1)}(\Delta t)^{1/2}$ should be larger than $\sqrt{N_x^{(0)}}$ in a typical experimental time interval Δt, and this process does not need an image of high quality at $\Delta s'$. Contrarily, if the FM is laid at an obvious nonsymmetrical plane, then it is difficult to focus the photon fluxes due to the spread property of the GB (see Fig. 9).

(3) The photon fluxes $N_z^{(0)}$ and $N_z^{(1)}$ in the z direction have a similar property. However, unlike the relation between $N_x^{(0)}$ and $N_x^{(1)}$, $N_z^{(0)}$ (noise) is much larger
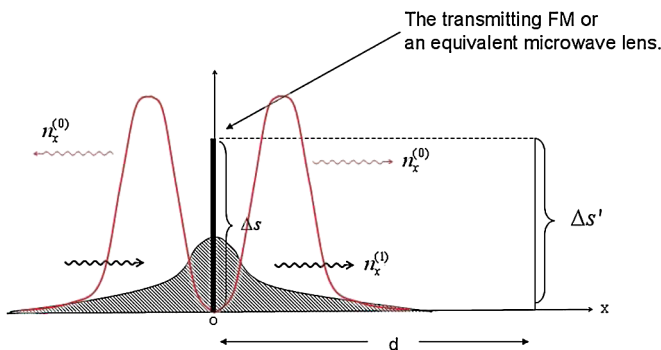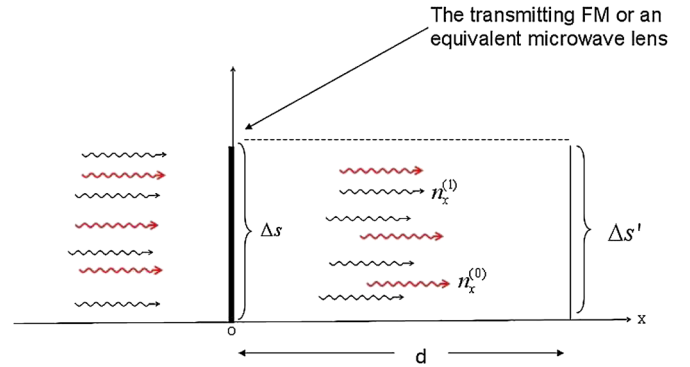

FIG. 8 (color online).   If the FM is just laid at the yz plane or at the parallel planes very near the yz plane, then the wave fronts of the photon fluxes passing through the planes would be the plane or the pseudoplane, and it is possible to obtain an effective focusing effect.

than $N_z^{(1)}$ (signal) in almost all of the regions. This is a very important difference between the photon fluxes in two such directions.

(4) A major role of the FM or other equivalent micro-wave lenses in the scheme is their focusing effect and not their superconductivity, and this does not mean that one can measure only $N_x^{(1)}$ ("interference term") and not $N^{(0)}$ (background). Also, it does not mean that $N^{(0)}$ is neglected and $N^{(0)}$ does not reach the photon flux detector. Actually, the FM is immersed in the BPF. Thus the BPF will generate the thermal noise in the FM. However, the BPF itself and the thermal noise photons caused by the BPF in the FM have an essential difference. The former is a vector and has high directivity; the latter are photons of random thermal motion. Under the low-temperature condition, the latter are much less than the former. In particular, $N_z^{(0)}$ and $N_y^{(0)}$ of the BPF are exactly parallel to the yz plane and exactly perpendicular to $N_x^{(0)}$ and $N_x^{(1)}$. Thus $N_z^{(0)}$ and $N_y^{(0)}$ do not provide any direct contribution to the photon

FIG. 7 (color online).   Unlike the photon fluxes $N_z^{(0)}$ and $N_z^{(1)}$, $N_x^{(1)}|_{x=0} = N_x^{(1)}|_{\max}$, where $N_x^{(0)}|_{x=0} = 0$. This means that $N_x^{(0)}$ and $N_x^{(1)}$ focused by the FM at the yz plane or at the parallel planes very near the yz plane would have a good focusing effect and SNR.
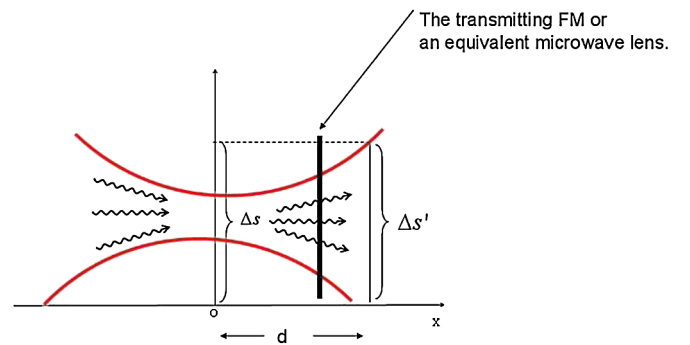
FIG. 9 (color online).   If the FM is laid at an obvious nonsymmetrical plane, then it is difficult to focus the photon fluxes due to the spread property of the GB.

flux passing through the receiving surfaces parallel to the yz plane, nor are they reflected, transmitted, or focused by the FMs laying at the receiving surfaces. In other words, the photon flux focused by the FM will be $N_x^{(0)}$, $N_x^{(1)}$ and not $N_z^{(0)}$, $N_y^{(0)}$. In this case $N_x^{(1)}$ and $N_x^{(0)}$ would reach simultaneously the detector, but $N_x^{(1)}$ and $N_x^{(0)}$ in the different receiving surfaces have the different ratio $N_x^{(1)}/N_x^{(0)}$; this is an important difference to the plane EMW case. Therefore, it is always possible to choose a best region and the receiving surface to detect the total photon flux $(N_x^{(0)} + N_x^{(1)})$ which has a good SNR. Furthermore, the $N_x^{(0)}$ can be differentiated from the $N_x^{(1)}$ by modulating the $\hat{B}_y^{(0)}$.

E. Challenge and issues

Except for the above-principle analysis, of course, one must consider the following challenge and issues. They would include the generation of a high-quality GB, suppression of the noises, such as thermal noise, the radiation press noise, and noises caused by the scattering of photons, dielectric dissipation due to the dust and other particles, and the concrete influence and correction of the FMs to the GB itself, etc.

The low-temperature $(T \sim 1 \text{ K}$ or less) and vacuum operation can effectively reduce the thermal noise and dielectric dissipation. There is room for improvement in other ways as well. They would include utilization of superstrong static magnetic fields, matching of ultrahigh sensitivity microwave photon detectors, construction of a good "microwave darkroom," coupling between the open superconducting cavities and the current scheme (the open superconducting cavities have a very large quantity factor $Q \sim 10^9$–10^{11}, and this coupling might greatly enhance the signal photon flux and not increase obviously the noise power), etc. All of these issues need further theoretical study and careful experimental investigation, and they would provide new ways and possibilities to further narrow the gap between the detection schemes and the reality of a valid measurement.

V. BRIEF SUMMARY

The EM detecting scheme based on the pure inverse G effect in the laboratory would not be capable of detecting the HFGWs in the gigahertz band, while the coupling system among the Gaussian-type microwave photon flux, the static magnetic field, and the fractal membranes (or other equivalent microwave lenses) will be a useful candidate. The key parameter in the current scheme is not the second-order PPF but the transverse first-order PPF; the measurable photon flux is not only the transverse first-order PPF but the total transverse photon flux, and they have different SNRs at the different receiving surfaces; the requisite minimal accumulation time Δt of the signal at the special receiving surfaces and in the background photon flux noise would be $\sim 10^3$–10^5 s for the typical laboratory condition and the parameters of $\hat{h} \sim 10^{-26}$–$10^{-30}/\sqrt{\text{Hz}}$ at $\nu = 5$ GHz with bandwidth ~ 1 Hz.

This paper does not involve the standard quantum limit (SQL) caused by the quantum backaction. The SQL constrains the possible sensitivity limit. We shall show that the SQL in the current scheme does not constrain predicated sensitivity (including the constant amplitude HFGWs and the stochastic high-frequency relic GWs). In other words, the sensitivity in the current scheme is the photon signal limited, not quantum noise limited [46]. We will discuss relative issues elsewhere.

ACKNOWLEDGMENTS

[1] R. L. Forward and R. M. L. Baker, Lockheed Astrodynamics Research Center, 650 N. Sepulveda, Bel Air, CA, USA, Lockheed Research Report No. RL 15210, 1961 (Forward coined the term "high-frequency gravitational waves").

[2] M. E. Gertsenshtein, Sov. Phys. JETP **14**, 84 (1962).

[3] L. Halpern and B. Laurent, Nuovo Cimento **33**, 728 (1964).

[4] R. A. Isaason, Phys. Rev. **166**, 1263 (1968).

[5] R. A. Isaason, Phys. Rev. **166**, 1272 (1968).

[6] L. P. Grishchuk and M. V. Sazhin, Sov. Phys. JETP **32**, 213 (1974).

[7] L. P. Grishchuk and M. V. Sazhin, Sov. Phys. JETP **41**, 787 (1975).

[8] G. F. Chapline, J. Nuckolls, and L. L. Wood, Phys. Rev. D **10**, 1064 (1974).

[9] V. B. Braginsky and V. N. Rudenko, Phys. Rep. **46**, 165 (1978).

[10] S. W. Hawking and W. Israd, *General Relativity: An Einstein Centenary Survey* (Cambridge University Press, Cambridge, England, 1979), pp. 90–137.

[11] M. Giovannini, Phys. Rev. D **60**, 123511 (1999).

[12] M. Giovannini, Classical Quantum Gravity **16**, 2905 (1999).

[13] A. Riagudo and J. P. Ugan, Phys. Rev. D **62**, 083506 (2000).

[14] M. Giovannini, Phys. Rev. D **73**, 083505 (2006).

[15] M. Giovannini, arXiv:0807.4317.

[16] J. E. Lidsey *et al.*, Phys. Rep. **337**, 343 (2000).

[17] M. Gasperini and G. Veneziano, Phys. Rep. **373**, 1 (2003).

[18] G. Veneziano, Sci. Am. **290**, 30 (2004).

[19] G. S. B. Kogan and V. R. Rudenko, Classical Quantum Gravity **21**, 3347 (2004).

[20] R. M. L. Baker, R. C. Woods, and F. Y. Li, AIP Conf. Proc. **813**, 1280 (2006).

[21] P. Chen, Mod. Phys. Lett. A **6**, 1069 (1991).

[22] A. I. Nikishov and V. I. Ritus, Sov. Phys. JETP **69**, 876 (1989).

[23] A. I. Nikishov and V. I. Ritus, Sov. Phys. JETP **71**, 643 (1990).

[24] G. Gratta *et al.*, in *Workshop on Beam-Beam and Beam-Radiation Interaction; High Intensity and Nonlinear Effects, Los Angeles, USA, 1991*, edited by C. Pellegrini *et al.* (World Scientific, Singapore, 1992), p. 70.

[25] P. Chen, Stanford Linear Accelerator Center Report No. SLAC-PUB-6666, 1994.

[26] X. G. Wu and Z. Y. Fang, Phys. Rev. D **78**, 094002 (2008).

[27] A. M. Cruise, Classical Quantum Gravity **17**, 2525 (2000).

[28] A. M. Cruise and R. M. J. Ingley, Classical Quantum Gravity **22**, S479 (2005).

[29] R. Ballantini *et al.*, arXiv:gr-qc/0502054.

[30] R. Ballantini *et al.*, Classical Quantum Gravity **20**, 3505 (2003).

[31] A. Nishigawa *et al.*, Phys. Rev. D **77**, 022002 (2008).

[32] F. Y. Li, R. M. L. Baker, Z. Y. Fang, G. V. Stepheson, and Z. Y. Chen, Eur. Phys. J. C **56**, 407 (2008).

[33] W. K. De Logi and A. R. Mickelson, Phys. Rev. D **16**, 2915 (1977).

[34] A. N. Cillis and D. D. Harari, Phys. Rev. D **54**, 4757 (1996).

[35] D. Boccaletti *et al.*, Nuovo Cimento B **70**, 129 (1970).

[36] L. D. Landau and E. M. Lifshitz, *The Classical Theory of Fields* (Nauka, Moscow, 1973), pp. 368–370.

[37] P. Chen, Phys. Rev. Lett. **74**, 634 (1995).

[38] M. Marklund, G. Brodin, and P. Dunsby, Astrophys. J. **536**, 875 (2000).

[39] V. De Sabbata *et al.*, Sov. J. Nucl. Phys. **8**, 53 (1969).

[40] A. Yariv, *Quantum Electronics* (Wiley, New York, 1975), 2nd ed., pp. 110–129.

[41] J. Li, F. Y. Li, and Y. H. Zhong, Chinese Phys. B **18**, 922 (2009).

[42] R. M. L. Baker (private communication).

[43] W. J. Wen *et al.*, Phys. Rev. Lett. **89**, 223901 (2002).

[44] L. Zhou *et al.*, Appl. Phys. Lett. **82**, 1012 (2003).

[45] B. Hou *et al.*, Opt. Express **13**, 9149 (2005).

[46] G. V. Stephenson, in *Proceedings of the Space, Propulsion and Energy Sciences International Forum (SPESIF)*, edited by Glen Robertson (paper 023), AIP Conf. Proc. Vol. 1103 (AIP, New York, 2009), pp. 542–547.